

Connection and performance of two-way CLT plates

Phase II

by

Chao (Tom) Zhang

Julian Asselstine

George Lee

Dr. Frank Lam

Prepared for

Forestry Innovation Investment

1130 W Pender St, Vancouver

BC V6E 4A4

Timber Engineering and Applied Mechanics

(TEAM) Laboratory

Department of Wood Science

Faculty of Forestry

University of British Columbia

Vancouver, B.C., Canada

March 25, 2019

Timber Engineering and Applied Mechanics (TEAM) Laboratory

#1901 - 2424 Main Mall, Vancouver, B.C. Canada V6T 1Z4; Tel: (604) 822-8137 Fax: (604) 822-9159

EXECUTIVE SUMMARY

In Phase I of *Developing Large Span Two Way CLT Floor System* (2017-18) we studied the performance of a steel plate connection system for the minor direction of CLT plates. The connected specimens had higher stiffness and strength compared to intact members under bending. In Phase II (2018-19) we designed and tested another connector based on Laminated Veneer Lumber (LVL). The bending stiffness of a joint was evaluated by the slip modulus between the connector plate and CLT under shear. The LVL based connector had 87% of the stiffness compared to the steel plate connector tested in Phase I, while performed much better at the initial period of the loading. Considering other factors, including manufacturing cost, assembly time, structural integrity, and fire protection, the LVL connection was found to be a good solution for joining the minor direction of CLT plates. An analytical model was proposed to establish the relationship between the slip modulus and the joint stiffness.

The connectors were loaded under in-plane shear to investigate the diaphragm behavior. The result indicated that two stiffness stages occurred: a high stiffness in the beginning (56.8 kN/mm) and after reaching a transitional load, a prolonged low stiffness region (4.3 kN/mm). The stiffness associated with the initial period was recommended for use in design. The joined panel remained fairly rigid as a two way plate under most circumstances, due to the high in-plane stiffness at the joint.

In Phase I and Phase II, four CLT panels were tested to measure the deflections in two way bending action. The single panel had a size of 3.66 m by 1.83 m, while the joined panels were 3.66 m by 3.66 m. By doubling the length in the minor direction, the maximum deflection at the center also doubled, from 5.87 mm to 12 mm. At the same time, the principle deflection changed from the major direction to the minor direction. Attaching two Parallel Strand Lumber (PSL) rim beams along the minor direction reduced the maximum deflection from 12.00 mm to 9.49 mm, a reduction of 21%, which corresponded approximately to the amount of EI increased in the minor direction. If the maximum load applied was uniformly distributed over the joined panel, the pressure was 3.45 kPa while the maximum deflection was 1/280 of the span (1/354 for the panel with rim beams).

A model using the crossing beam method was developed to estimate the two way panel deflection with column supports. The estimated deflection was in the range of 87-108% of the measure value. The model predicted the contribution of the rim beams with good accuracy. Ongoing study is being conducted using Finite Element Method to simulate the two way action. Other issues related to the application of continuous two way CLT plate were also discussed, including working with concrete topping, installation procedure, lifting technique, and connection with other structural elements. The preliminary results of some ongoing work were presented briefly with future work recommended.

TABLE OF CONTENT

EXECUTIVE SUMMARY 2

Table of Content 3

List of Tables 5

List of Figures 4

1 Introduction 6

2 Material and Methods 6

 2.1 Connection test..... 7

 2.2 Diaphragm test 9

 2.3 Joined panel test..... 11

3 Results and Discussions..... 14

 3.1 Connection test..... 14

 3.2 Diaphragm test 18

 3.3 Joined panel test..... 20

4 Conclusions and recommendations 25

 4.1 Connection performance 25

 4.2 Diaphragm behavior..... 26

 4.3 Joined panel deflection 27

 4.4 Assembling and lifting..... 27

5 Acknowledgements 28

6 References 28

Appendix A Joined panel test results..... 29

LIST OF FIGURES

Figure 1 Moment applied on a steel plate based connection 8

Figure 2 Moment applied on an LVL based connection..... 8

Figure 3 H-block test for joint connections 9

Figure 4 Diaphragm performance of a joined panel 10

Figure 5 Setup for diaphragm test..... 10

Figure 6 Joined CLT panel and the lifting platform 11

Figure 7 Transducer locations for the joined panel test..... 12

Figure 8 Loading of the joined panel..... 13

Figure 9 Rim beam attached to the edge of the joined panel..... 13

Figure 10 Screws to attach rim beams to the panel 13

Figure 11 CLT failure in the H-block connection test..... 15

Figure 12 Beam deformation under bending 16

Figure 13 Deformation at the joint under bending..... 16

Figure 14 Analytical model of deformation at the joint 17

Figure 15 Diaphragm test results 19

Figure 16 Deformation of connectors in diaphragm test 20

Figure 17 Comparison of displacement in the major direction..... 21

Figure 18 Comparison of displacement in the minor direction 22

Figure 19 Center displacement for four panels tested 22

Figure 20 Principle and non-principle directions under loading 23

Figure 21 Beam strip and column strips for deflection calculation 24

Figure A- 1 Displacement of the joined panel in the major direction 29

Figure A- 2 Displacement of the joined panel in the minor direction 29

Figure A- 3 Displacement of the joined panel with rim beams in the major direction..... 30

Figure A- 4 Displacement of the joined panel with rim beams in the minor direction 30

LIST OF TABLES

Table 1 Material list 6

Table 2 Comparison of steel plate based and LVL based connections..... 14

Table 3 Comparison of estimated rotational stiffness results 18

Table 4 Stiffness and load of diaphragm test specimens 19

Table 5 Deflection along the major direction under maximum load 21

Table 6 Deflection along the minor direction under maximum load..... 21

Table 7 Estimated panel deflections 25

1 INTRODUCTION

Cross Laminated Timber (CLT) is treated as one way bending element under the current design method. The rigid CLT plates are supported by drop beams or sometimes columns if the span is short enough. In both cases, the clear floor space is quite limited. In massive timber construction architects are often seeking to create large span open space. CLT has the potential to provide an efficient solution if the two way bending action is considered.

Phase I of this project studied the connections used to join multiple CLT plates in the minor direction (*TEAM Report 2017-08*). The connectors were based on slotted steel plate and self-tapping wood screws. The connected beams had higher stiffness and higher strength than the intact specimens. Phase II studied an improved connection system, the diaphragm behavior of connectors, the two way bending action of a joined panel, and the effect of rim beams in stiffening the panel. Analytical models were developed to estimate the connection stiffness and the two way panel deflection.

2 MATERIAL AND METHODS

The material used in this project is shown in Table 1. The CLT was E1M5 175E 5 layer, manufactured by Structurlam Products Ltd. (Penticton, BC). The lumber in the major direction layers was MSR 2100 1.8E Spruce-Pine-Fir (SPF), and the lumber in the minor direction layers was SPF #2 & Better. The Laminated Veneer Lumber (LVL) was LP SolidStart® 2950Fb-2.0 E (13.8 GPa). The Parallel Strand Lumber (PSL) was Trus Joist Parallam 2.0 E Douglas Fir manufactured by Weyerhaeuser. The screws, washers, and pre-drilling jig were made by SWG Schraubenwerk Gaisbach GmbH (Waldenburg, Germany)..

Table 1 Material list

Item	Description
CLT	E1M5 175 E 5 layer, 175 mm thick
LVL	2950Fb-2.0 E
PSL	2.0E Douglas fir
Screws	ASSY Plus VG screws 12×160, CSK head, milling pocket; ASSY Plus VG screws 12×200, CSK head, milling pocket; ASSY Plus VG screws 10×160, CSK head, milling pocket;
Washers	45° washers for 12 mm countersunk screw head
Steel plate	A36, 6.4 mm thick, 127 mm wide, slotted
Pre-drilling jig	For 12 mm screws at 45°

The connection test studied the feasibility and performance of an LVL-based connection compared to the steel plate based connection used in Phase I. This connection was chosen amongst multiple designs tested, with the objective to maintain the same level of stiffness,

but at a lower cost as well as shorter installation time compared to the steel solution in Phase I. The diaphragm test investigated the behavior of the connection under in-plane loading, which was also a critical issue for the continuous two way panel. Then two CLT plates were joined together with LVL-based connections and supported at the four corners. Concentrated load was applied at the center of the joint panel and its deflection measured at different loading levels. Two configurations were compared: one without rim beams, and the other with two rim beams installed at the edge along its minor direction.

2.1 Connection test

In Phase I the steel plate based connection was found to be effective in connecting CLT in the minor direction. With sufficient number of connections, the joined CLT plate had higher stiffness and strength than the intact panel. The cost of this connection system was relatively high since it involved slotted steel plates and cast iron screw washers. At installation, predrilling is required for the screws so that the washers could fit well with the slots. Therefore, a better solution was needed to reduce the cost and speed up the installation process.

LVL based connection was chosen amongst multiple designs tested. This connection replaced the steel plate with 40 mm thick LVL plate. Countersunk head self-tapping wood screws were driven directly into the wood in 45° angle without predrilling. LVL had a higher density providing good head pull-through and withdrawal resistance. The veneer layup also prevented wood splitting occurred in other types of high density wood product.

In an intact panel, the moment on a cross section was resisted by the longitudinal layers (in the minor direction of a 5-layer CLT, 2nd layer from the top under compression and 4th layer under tension). For the cross section at the joint of a connected panel, as shown in Figures 1 and 2, the resistance on the tension side was provided by steel/LVL plates while on the compression side by both the lumber and steel/LVL plates. The stiffness and strength of the joint was largely determined by the performance of the connection under horizontal shear. Therefore, CLT and steel/LVL plates were assembled as an H-shaped specimen in order to quantify the connection stiffness, as shown in Figure 3. Four screws (ϕ 12 mm, 160 mm long) were installed in two rows on each side member. The load was applied on the center member at a rate of 0.8 mm/min. Two transducers were installed to measure the relative displacement between CLT and side members. Fifteen replicates were tested for each type of connection. The stiffness and strength of every specimen were calculated based on the measurements.

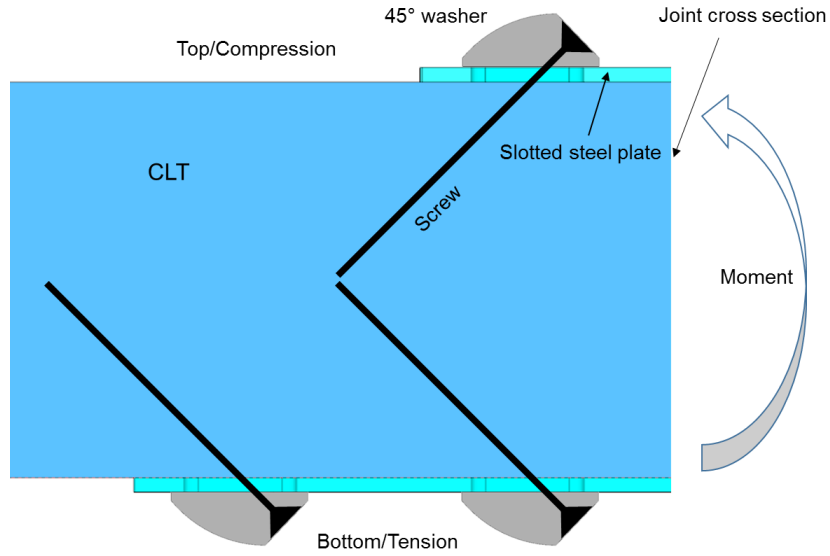


Figure 1 Moment applied on a steel plate based connection

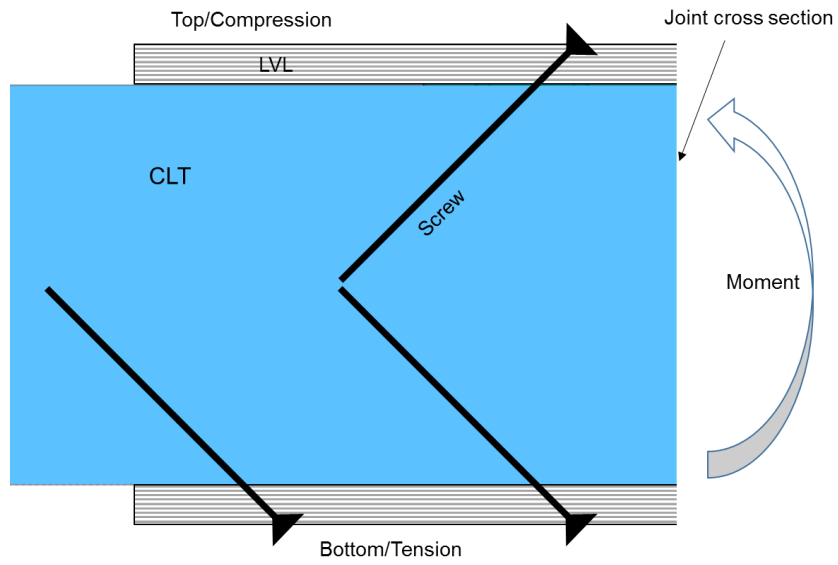


Figure 2 Moment applied on an LVL based connection



Figure 3 H-block test for joint connections

2.2 Diaphragm test

The diaphragm performance of a large span CLT plate is critical in a two way action, especially when supported by columns only. For a joined panel, the connectors had to resist the shear force along the joined edge created by the in-plane load transferred from adjacent structural components (beams or columns), as shown in Figure 4. The loading condition on the connector could be simulated by the test setup shown in Figure 5. The main member was loaded in the in-plane direction while the two side members were clamped to test fixtures to prevent rotation. Each side member was connected to the main member by two steel plates with four screws per plate. The screws were installed in 45° to the CLT surface. Two transducers were mounted on the main member to measure its displacement relative to the side members. The loading rate was 1.5 mm/min and five replicates were tested.

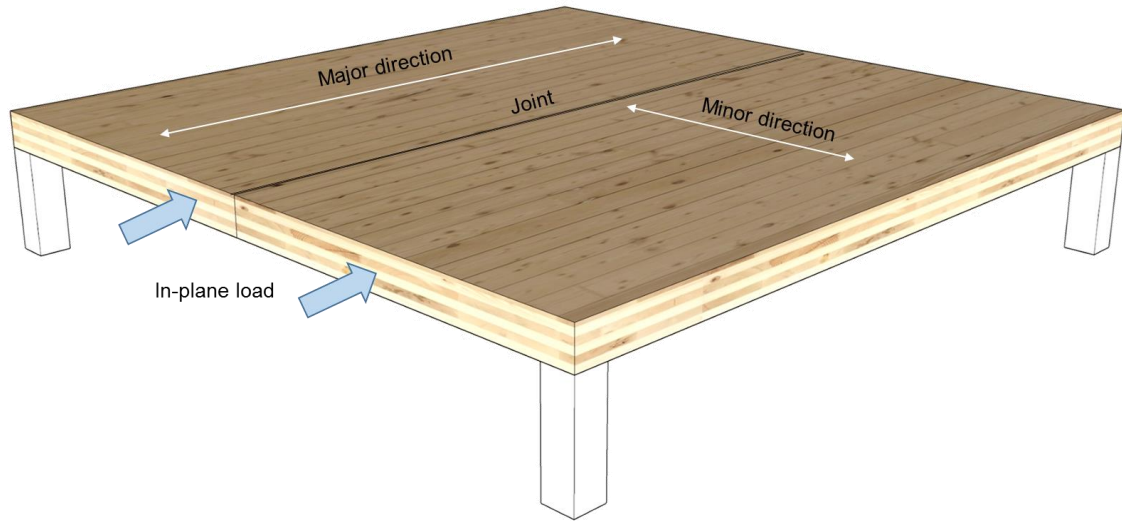


Figure 4 Diaphragm performance of a joined panel

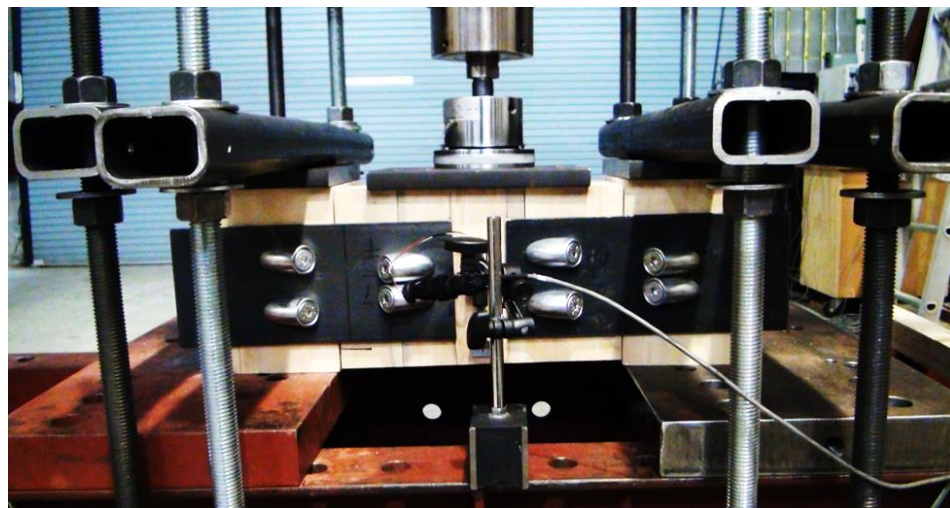
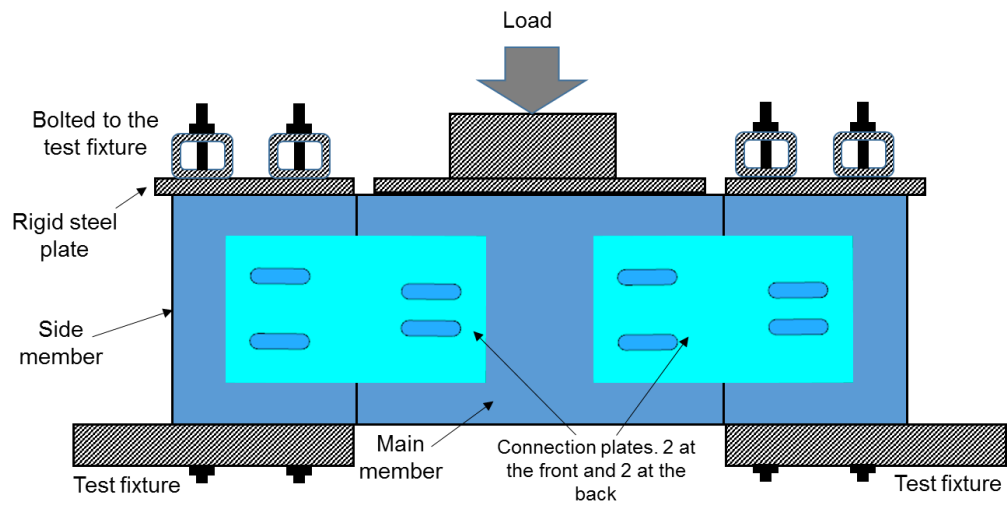


Figure 5 Setup for diaphragm test

2.3 Joined panel test

Two CLT panels were joined together in the minor direction using the connectors tested above. Each panel was 1.83 m (minor direction) by 3.66 m (major direction) and they had been loaded within the elastic range to measure the stiffness in Phase I of this project. Ten LVL plates and one steel plate were installed at the top (compression side) with four screws on each plate. Sixteen LVL plates and two steel plates were installed at the bottom (tension side) with eight screws on each plate.

Two steel beams with PSL spacers in between were used to create a platform for lifting and installation. The four ends of the beams were attached to the crane. Initial gaps between panels were closed with tie-down straps. Steel plates were installed at the center, and LVL plates were evenly located towards the edges except near the supporting beams. The lifting platform and installation techniques were found to be efficient.

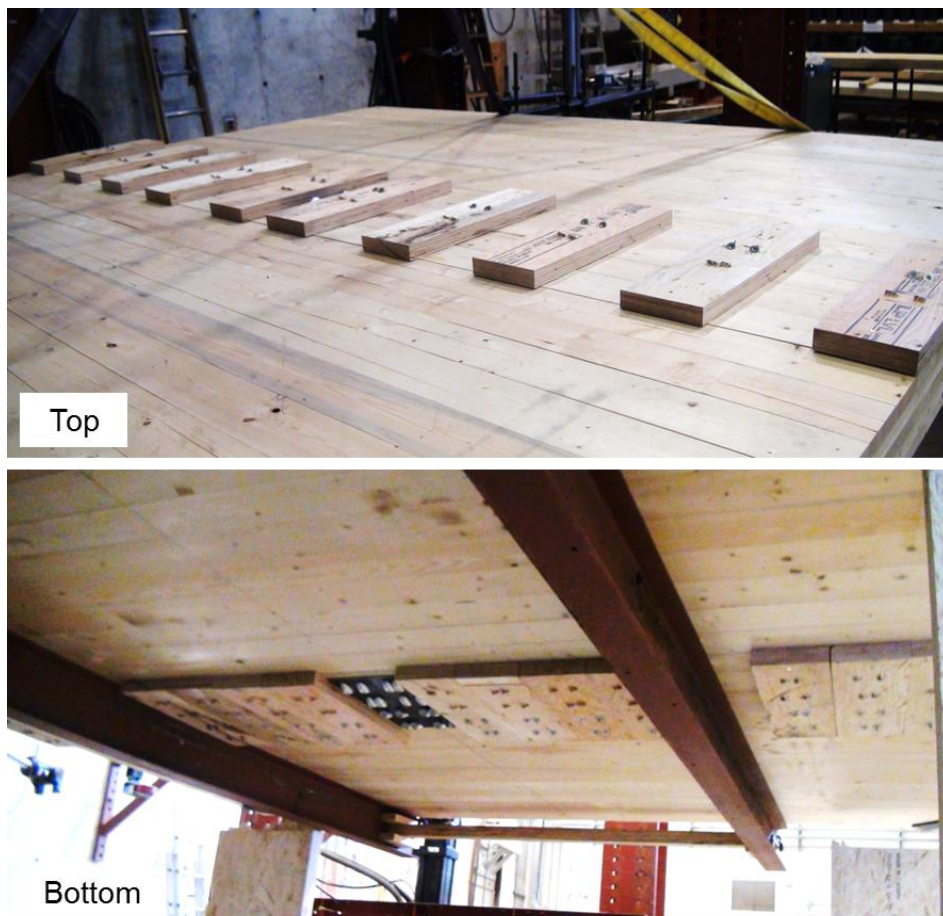


Figure 6 Joined CLT panel and the lifting platform

The joined panel was simply supported at its four corners, in a similar setup used in Phase I. The transducer locations are shown in Figure 7: nine were installed below the panel to measure the vertical deflection, and two were installed on yokes at the edge to measure the

center deflection relative to the supports. The load was applied evenly on two areas of 130 mm by 520 mm at the center, with 600 mm distance in between. This arrangement was due to the uneven surface at the top of connection plates. Five thick steel plates were used to load the panel, as shown in Figure 8. Each steel plate had a weight of 791.5 kg, equivalent to 7.76 kN. There was a 5 min interval between loading and unloading each plate to ensure the panel deflection had stabilized.

Afterwards two PSL beams were attached to the edges of the panel along its minor direction. The beam dimensions were 3.66 m × 175 mm × 63.5 mm (length × depth × width). In order to maintain sufficient shear force transfer between CLT and PSL beams, one set of Ø 10 mm × 160 mm screws was installed in 90°, and the other set of Ø 12 mm × 200 mm screws was installed in 45°. The spacing along the beam length was 305 mm (12 in) for both sets. This panel was loaded with the same protocol as above.

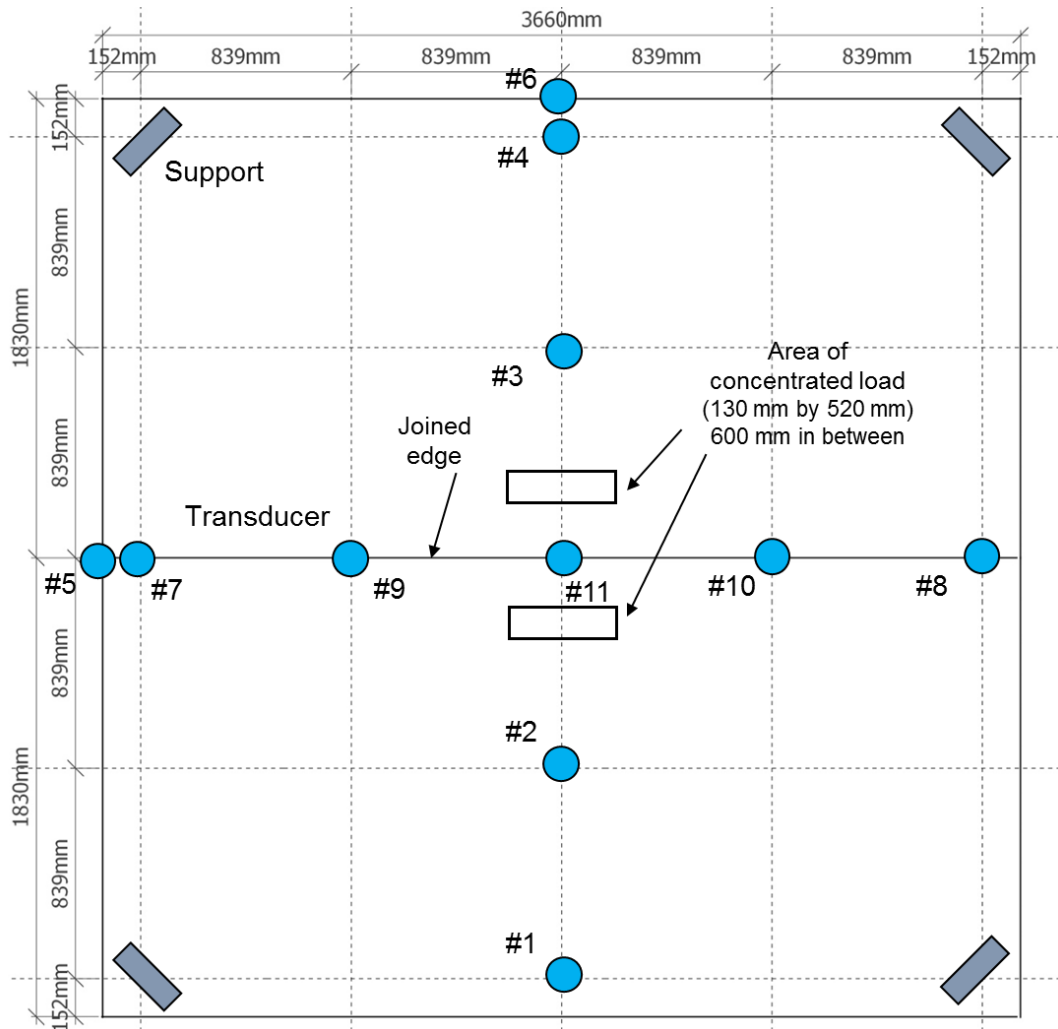


Figure 7 Transducer locations for the joined panel test



Figure 8 Loading of the joined panel



Figure 9 Rim beam attached to the edge of the joined panel

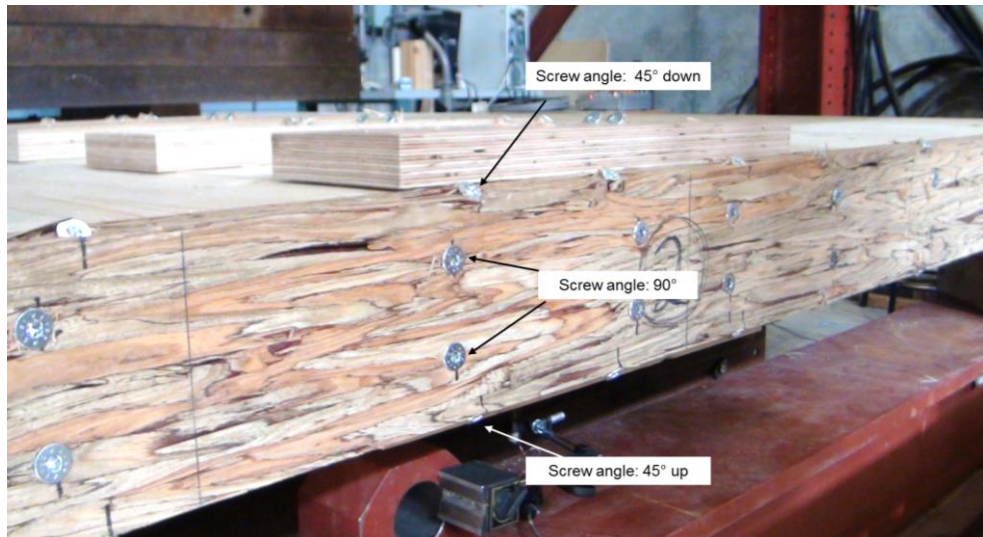


Figure 10 Screws to attach rim beams to the panel

3 RESULTS AND DISCUSSIONS

3.1 Connection test

The H-block test results for the steel plate connections and LVL connections are shown in Table 2. The slip modulus K (in kN/mm) was calculated as the slope of load-displacement curve between 15% and 50% of the peak load. This was a measurement of the relative displacement between CLT and the connection plate under shear. The coefficient of variation was in the same range: 23-24% for slip modulus and 7-9% for peak load. The average K of the LVL connections was 92.5 kN/mm, 87% of the average K of the steel connections. The difference of peak load was greater, with the LVL connection at 70% of the steel connection capacity. Most steel plate connections had a low stiffness range at the initial period of loading, probably due to closing the existing gaps between washers and slots. LVL connection engaged the load immediately from the start. Since the large span panel design was deflection controlled, the LVL connection was found to be a good alternative to steel connections.

The two types of connections failed in the same way, as shown in Figure 11, involving wood failure under tension perpendicular to grain, and glue-line failure at the corner of a laminae. This observation corresponded to the failure mode found in the bending test in Phase I.

Table 2 Comparison of steel plate based and LVL based connections

Item	Slip modulus K_o (kN/mm)			Peak load (kN)		
	LVL K_{ol}	Steel K_{os}	Ratio	LVL	Steel	Ratio
Average	92.5	106.5	87%	143.0	203.9	70%
Stdev	21.0	25.2	83%	10.6	17.9	59%
CV	23%	24%	96%	7%	9%	85%
Max	142.2	157.6	90%	161.3	238.9	68%
Min	63.9	61.9	103%	121.1	166.8	73%
Replicates	15	15	15	15	15	15

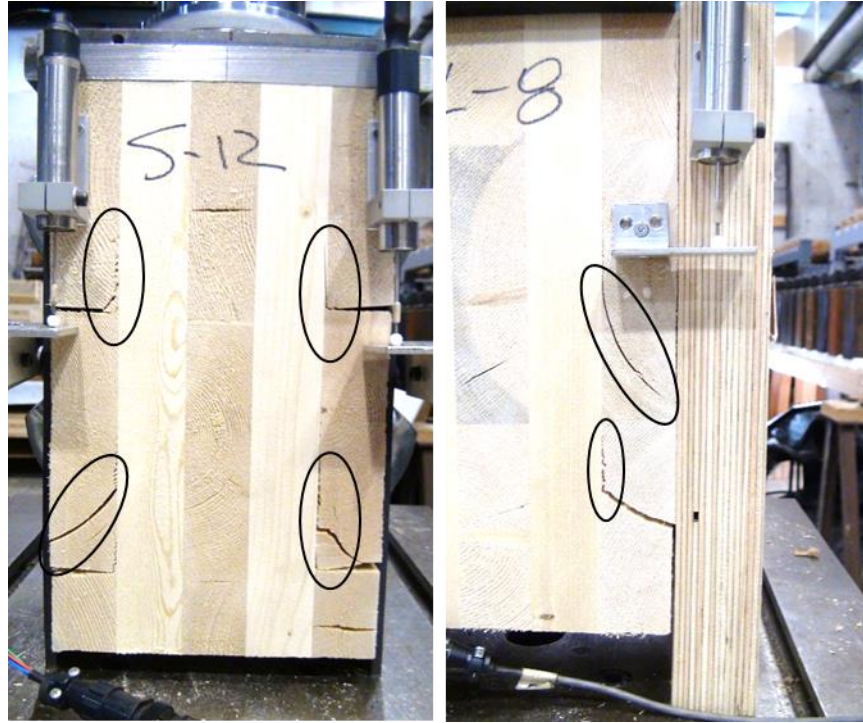


Figure 11 CLT failure in the H-block connection test

An analytical model based on simple beam theory was developed to compare the rotational stiffness of intact panels and joined panels. The part of beam investigated was the section with steel/LVL connectors (length l_c).

Figure 12 shows the deformation of a portion of beam under bending moment M . The angle between the two end sections is θ . The radius of curvature for this arch is defined as ρ . The relationship between θ and M can be expressed as:

$$\theta = \int_{x_1}^{x_2} \frac{1}{\rho} dx = \int_{x_1}^{x_2} \frac{M}{EI} dx \quad (1)$$

where: $EI=(EI)_{eff}$, the effective stiffness of the cross section.

Since M and EI are uniform in the portion of beam considered (shear free zone), Equation (1) could be simplified as:

$$\theta = \frac{M}{EI} \times l_c \quad (2)$$

where: l_c is the length of the steel plate working in the longitudinal (effective) layer.

The rotational stiffness for the intact panel, k_i (in kN m/rad), was estimated to be:

$$k_i = \frac{M}{\theta} = \frac{EI}{l_c} \quad (3)$$

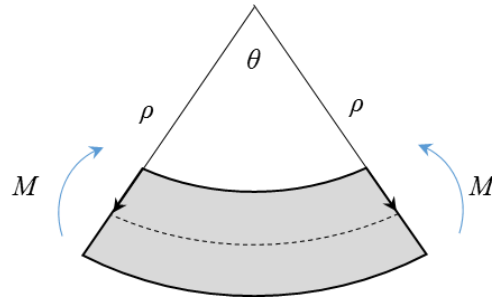


Figure 12 Beam deformation under bending

The deformation of a joint under bending is shown in Figure 13. The end surfaces of the longitudinal layers at the top (2nd layer from the top) firmly contacted, and wood was compressed. The only tension resistance came from the steel plate. As the steel plate shifted away from the CLT under shear, the angle between the two joined surfaces, θ' , increased, and it only occurred through the bottom three layers. The steel plate behaved as a spring with a stiffness of K_s (calculated from the slip modulus in Section 3.1). Based on these assumptions, an analytical model for the joint deformation is shown in Figure 14:

- F_{cs} : compressive force provided by the top steel plate;
- F_{cw} : the compressive force provided by the longitudinal lumber;
- F_t : the tensile force provided by the bottom steel plate;
- h_t : the distance between F_t and the center of rotation;
- E_w : the modulus of elasticity for longitudinal lumber.



Figure 13 Deformation at the joint under bending

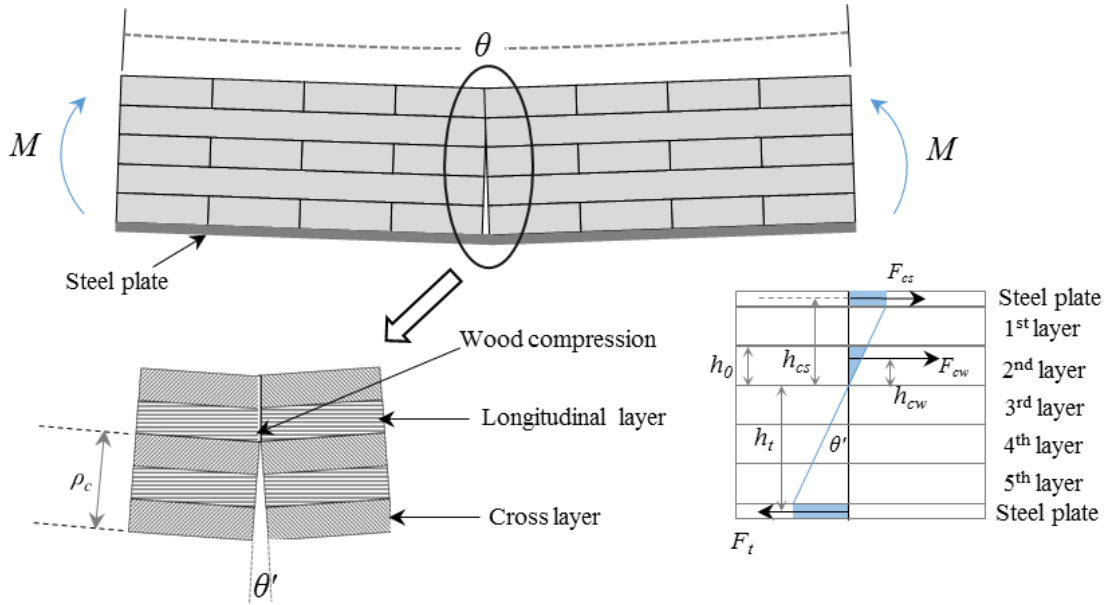


Figure 14 Analytical model of deformation at the joint

The correlation between the slip modulus K_s and the angle θ' was established. The angle θ , between two end sections of the whole portion considered, was the same as θ' .

$$M = F_t \times h_t + F_{cw} \times h_{cw} + F_{cs} \times h_{cs} \quad (4)$$

$$\frac{F_t}{K_s} = \rho_c \times \theta' \quad (5)$$

$$F_{cw} = \frac{\theta' \times h_0}{l_c} \times E_w \times b \times h_0/2 \quad (6)$$

$$F_{cs} = F_t - F_{cw} = \theta' \times \left(\rho_c \times K_s - \frac{h_0^2 \times E_w \times b}{2 \times l_c} \right) \quad (7)$$

The rotational stiffness of the steel connection k_{cs} was calculated as:

$$k_{cs} = \frac{M}{\theta} = \rho_c \times K_s \times (h_t + h_{cs}) - \frac{h_0^2 \times E_w \times b}{2 \times l_c} \times (h_{cs} - h_{cw}) \quad (8)$$

The rotational stiffness of the LVL connection k_{cl} could be calculated in a similar way:

$$k_{cl} = \frac{M}{\theta} = \rho_c \times K_l \times (h_{tl} + h_{cl}) - \frac{h_0^2 \times E_w \times b}{2 \times l_c} \times (h_{cl} - h_{cw}) \quad (9)$$

where: K_l : the slip modulus of the LVL connection;

h_{tl} : the distance between tensile force provided by LVL plates F_{tl} and the center of rotation.

h_{cl} : the distance between compressive force provided by LVL plates F_{cl} and the center of rotation.

The slip modulus K_0 in Table 2 was measured for 8 screws in the same direction. The connected panel used 16 screws at the tension side (with two steel plates or LVL plates). Therefore:

$$K_s = K_{0s}/2 \tag{10}$$

$$K_l = K_{0l}/2 \tag{11}$$

The estimated rotational stiffness results based on Equations (8) and (9) are shown in Table 3. The steel plate connection had a rotational stiffness of 782 kN m/rad, 98% of the stiffness of an intact panel. The LVL plate connection had a lower stiffness, but still maintained at a level of 92% compared to the full panel. The analytical model above did not consider the reinforcing effect of screws to the wood, which would further strengthen the connected portion and lead to a higher actual stiffness than predicted, as found in Phase I.

Table 3 Comparison of estimated rotational stiffness results

Specimen	Intact panel	Steel plate connection	LVL connection
k (kN m/rad)	801	782	734
% of the intact panel	100%	98%	92%

3.2 Diaphragm test

Diaphragm test investigated the performance of connectors under in-plane loading. There were four connection plates on each specimen (two at the front and two at the back), with four screws on each plate. The test results are shown in Figure 15 and Table 4. The displacement was the average relative movement between the center member and side members. The five specimens behaved in a similar manner, with a high stiffness phase in the beginning (K_1) and then changing to a prolonged low stiffness (K_2) period. The load at the transition and the load at 15 mm displacement are also shown in Table 4. The average stiffness K_1 was 56.8 kN/mm, and the average K_2 was 4.3 kN/mm. This decreasing of stiffness was quite drastic.

The deformation of the connectors is shown in Figure 16. The load on the screw was perpendicular to its shank and the reaction was mainly provided by the compression of wood. If higher stiffness is needed, the screws could be set in 45° in order to engage the withdrawal stiffness.

For a joined panel with the same number of connectors as used in Section 2.3, the stiffness of the connection under in-plane loading was estimated (other factors not considered) to

be: $K_1 = 667 \text{ kN/mm}$, $K_2 = 50.5 \text{ kN/mm}$, and the transitional load was 535.8 kN . The initial stiffness was equivalent to 182 kN/mm/m . Therefore, in most circumstances, the design of a joined two-way panel would be controlled by out of plane loading.

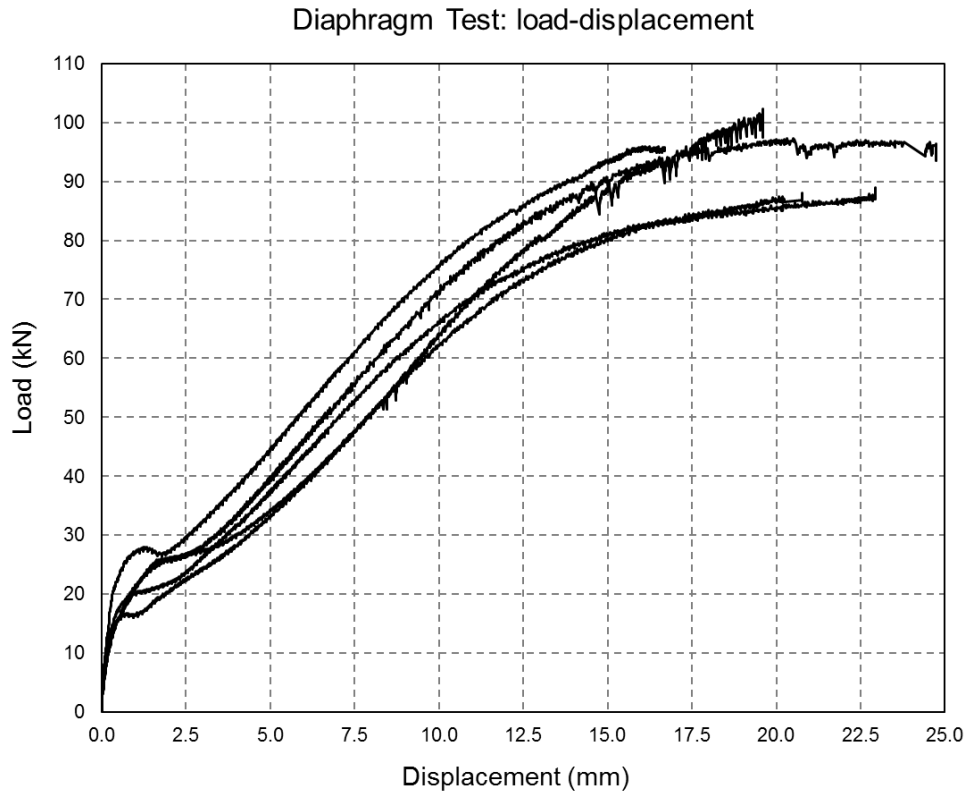


Figure 15 Diaphragm test results

Table 4 Stiffness and load of diaphragm test specimens

Specimen	Stiffness K_1 (kN/mm)	Load at transition (kN)	Stiffness K_2 (kN/mm)	Load at 15 mm (kN)
#1	61.0	16.2	6.8	92.2
#2	41.9	25.4	3.3	77.9
#3	60.1	26.7	3.5	91.6
#4	44.4	25.6	4.2	88.9
#5	76.6	20.1	3.6	80.0
Average	56.8	22.8	4.3	86.1
CoV	25%	20%	34%	8%



Figure 16 Deformation of connectors in diaphragm test

3.3 Joined panel test

This test measured the deflection of the joined panels under out of plane concentrated loading, in order to quantify the stiffness and to provide data for further modeling. The deflections at different locations under applied load levels are shown in Appendix A. The maximum deflections (at the center) of the panels tested in Phase I and Phase II are compared in Tables 5-6 and Figures 17-18. The four specimens had the same length in the major direction. The length of the single panels in the minor direction was half of the length of the joined panels.

The deflection of the joined panel at the center was about two times of the deflection in a single panel. The difference was greater towards the edges. Adding rim beams increased the stiffness and reduced the deflection by about 21%. The reduction corresponded approximately to the amount of increasing in EI in the minor direction. The maximum deflection of the joined panel was 12.0 mm, equivalent to $1/280$ of the span, while the maximum deflection of the joined panel with rim beams was equivalent to $1/354$ of the span. If the concentrated load was uniformly distributed over the panel, the load pressure would be 3.45 kPa and the corresponding deflection would become smaller than the above.

The center displacements for the four panels under different loading levels are shown in Figure 19. The joined panel had a slope of 3.23 kN/mm, and the joined panel with rim beams had a slope of 4.10 kN/mm (27% higher). The slope of the two single panels was in the range of 6.37-6.69 kN/mm.

Table 5 Deflection along the major direction under maximum load

Panel tested	Location along the major direction				
	Edge	Quarter	Center	Quarter	Edge
Single panel #1	1.85	4.32	5.76	3.93	0.53
Single panel #2	2.07	4.58	5.98	4.07	0.63
Joined panel (A)	10.13	11.22	12.00	11.19	10.55
Joined panel with rim beams (B)	7.10	8.60	9.49	8.55	7.37
Ratio: B/A	70%	77%	79%	76%	70%

Table 6 Deflection along the minor direction under maximum load

Panel tested	Location along the minor direction				
	Edge	Quarter	Center	Quarter	Edge
Single panel #1	4.76	5.42	5.76	5.42	4.90
Single panel #2	4.75	5.43	5.98	5.59	5.24
Joined panel (A)	3.85	9.27	12.00	8.93	3.38
Joined panel with rim beams (B)	3.09	7.38	9.49	7.16	2.77
Ratio: B/A	80%	80%	79%	80%	82%

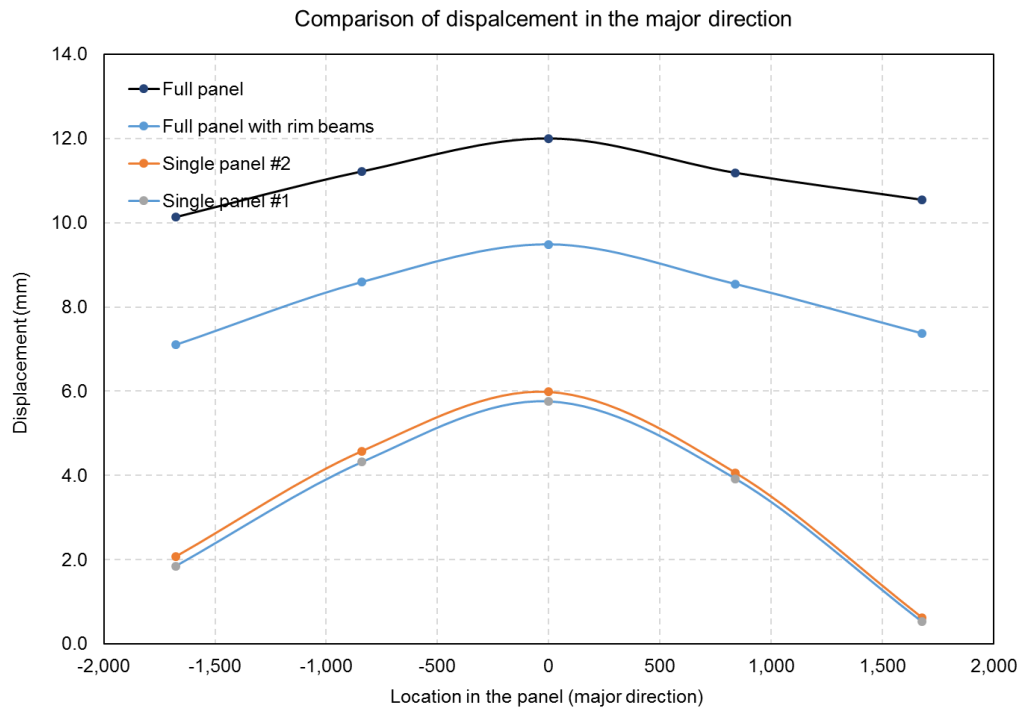


Figure 17 Comparison of displacement in the major direction

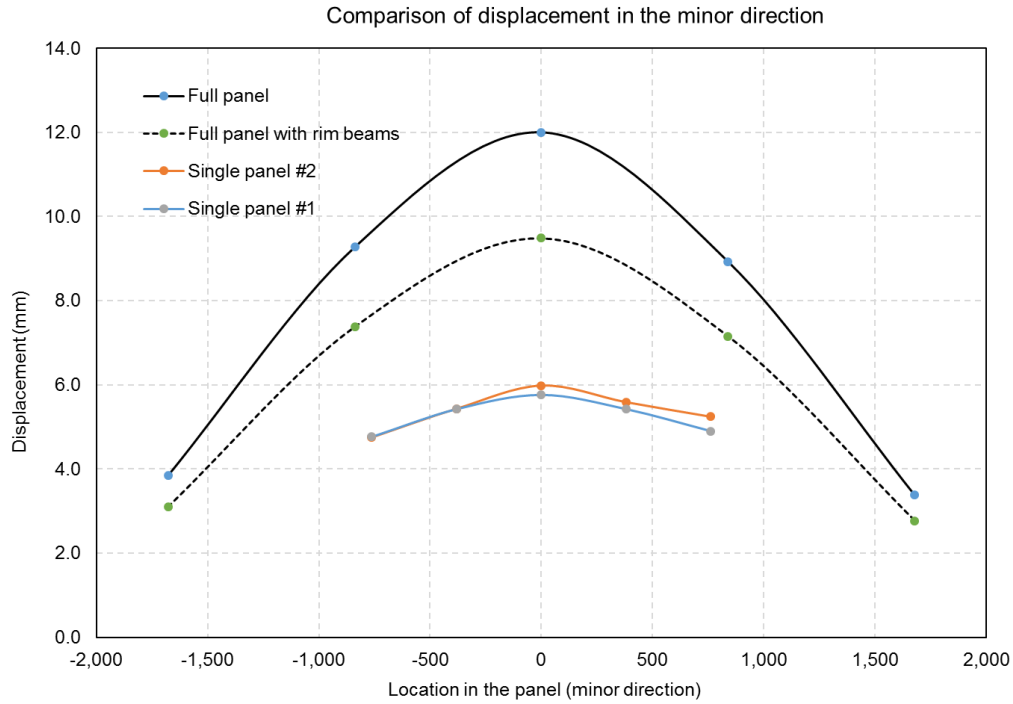


Figure 18 Comparison of displacement in the minor direction

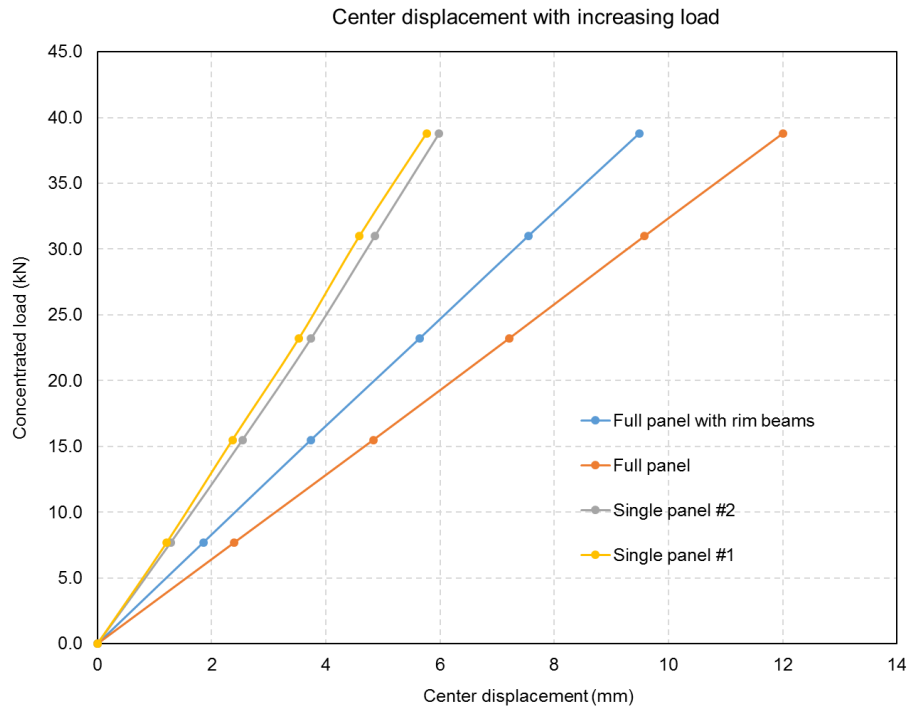


Figure 19 Center displacement for four panels tested

An ongoing study is being conducted using Finite Element Method to simulate the above connections as well as the two-way behavior of CLT panels. Here an analytical model was proposed to estimate the panel deflection based on the crossing beam method (works best

for uniformly distributed load over the panel). The support and loading conditions were the same as used in the test: column support at four corners with 38.5 kN loaded at the center. The joined panel had the same EI as the intact panel in the minor direction, based on results found in Phase I and Section 3.1.

The deflection of a beam under concentrated loads was a function of span l and stiffness EI :

$$\Delta \propto \beta = \frac{l^3}{EI} \tag{12}$$

The β values for the major direction (β_a) and minor direction (β_b) can be calculated, and the ratio γ is defined as:

$$\gamma = \frac{1/\beta_a}{1/\beta_b} \tag{13}$$

γ estimates the ratio of actual bending stiffness (P/Δ) in the two directions. This ratio could determine the principle direction, in which the main deflection occurred. For example, for the single panel in Table 5, $\gamma_s = 0.16$, meaning the main deflection occurred in the major direction. While for the joined panel, $\gamma_j = 3.79$, meaning the principle direction was the minor direction. The two directions are shown in Figure 20. Due to the large difference of P/Δ in the two directions (4-6 times), the panel could be treated as a long and narrow plate with a load applied in the center.

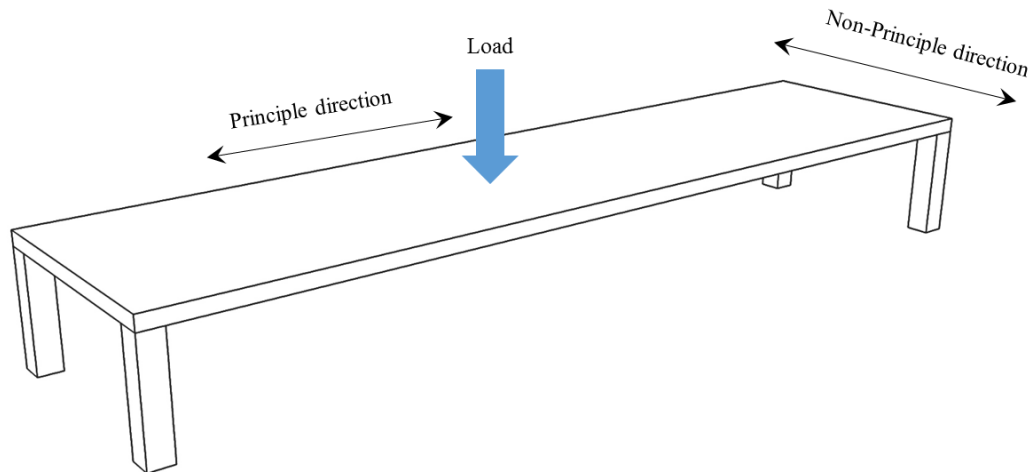


Figure 20 Principle and non-principle directions under loading

First the panel was assumed as a beam strip in the principle direction simply supported at the edges, and then the reaction at the edges was applied on two column strips, which were also considered as simply support beams, as shown in Figure 21. Due to the narrow width of the beam strip, the load was considered as uniformly distributed along its width. The

reaction load was assumed to be uniformly distributed on the surface of the column strip. The width of the column strip was estimated by the stiffness ratio γ :

$$b_{cs} = b \times \gamma_s \text{ or } b/\gamma_j \tag{14}$$

where: b is the width of length along the principle direction.

The effective stiffness EI were $(EI)_{a,eff}$ and $(EI)_{b,eff}$ for the major direction and minor direction, respectively. The center deflections of the beam strip and column strip can be calculated, as Δ_{bs} and Δ_{cs} , respectively:

$$\Delta_{bs} = \frac{w_{bs} l_{bs}^4}{\alpha_1 (EI)_{bs}} \tag{15}$$

$$\Delta_{cs} = \frac{w_{cs} l_{cs}^4}{\alpha_2 (EI)_{cs}} \tag{16}$$

where: α_1 and α_2 are constants depending on the load distribution pattern;
 $(EI)_{bs}$ is the effective stiffness of the beam strip;
 $(EI)_{cs}$ is the effective stiffness of the column strip.

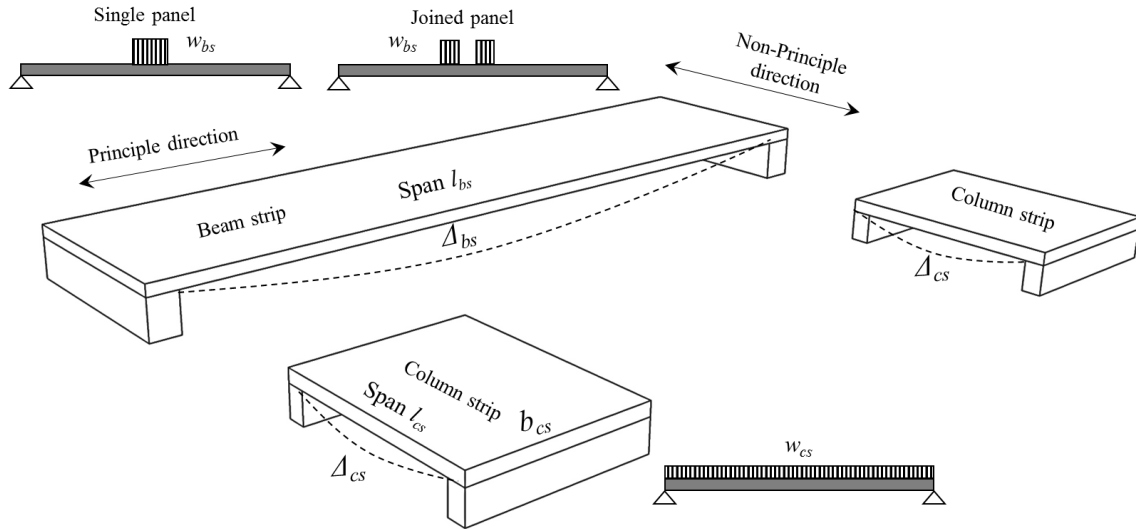


Figure 21 Beam strip and column strips for deflection calculation

For the joined panel with rim beams, the column strip had a higher EI since it was reinforced by the attached PSL.

The deflection at the center of the panel was:

$$\Delta = \Delta_{bs} + \Delta_{cs} \tag{17}$$

The estimated maximum deflections under an applied load of 38.5 kN are shown in Table 7. The largest discrepancy occurred in the joined panel without rim beams, with 13% difference. It captured the strengthening effect of the rim beams, yielding a reduction of 18% in deflection. This analytical model was a first step to establish a design approach for two-way CLT panels. Further optimization is needed in combination with the Finite Element Method results.

Table 7 Estimated panel deflections

Specimen	Single panel #1	Single panel #2	Joined panel	Joined panel with rim beams
Estimated (mm)	6.20	6.20	10.42	8.58
Measured (mm)	5.76	5.98	12.0	9.49
Difference	108%	104%	87%	90%

4 CONCLUSIONS AND RECOMMENDATIONS

4.1 Connection performance

An improved connection based on the one used in Phase I was proposed and tested, with an objective to reduce the manufacturing cost and to speed up the installation process. Since the moment at the joint cross section was transformed into horizontal shear force between CLT and connecting plates. The performance of the two types of connectors was quantified and compared using an H-block test setup. Its shear resistance was represented by a slip modulus K . The LVL connectors had an average slip modulus of 92.5 kN/mm, at 87% of the steel plate connectors. The LVL connectors performed better at the initial part of the loading since they engaged the load immediately while the steel connectors took some time to close the existing gaps within. Although LVL connections had a lower peak load, it would not be a controlling factor in the design since the large span panel was mostly governed by deflection not by strength. The cost of a LVL connection is a fraction of the steel plate connection cost. It does not require predrilling and has a greater tolerance of inaccurate screw angles, leading to faster installation. In practice a large LVL plate could be used instead of many small plates, providing better structural integrity and fire protection. If a clean surface finish is needed, the connectors can be countersunk into the wood, as the surface layer of the minor direction is not counted as part of the effective cross section. Considering all the factors above, the LVL connection was found to be a better option thus recommended for future applications.

An analytical model was proposed to estimate the rotational stiffness at the connection, in order to compare a joined section with an intact section. The model was based on simple beam theory and the assumption that the rotation of a connected section was created by the slippage of tension plates relative to CLT. The slip modulus measured above was used to predict the rotational stiffness. The steel plate connection had a stiffness of 782 kN m/rad,

98% of the stiffness of an intact panel. The LVL plate connection had a lower stiffness, but still maintained at a level of 92% compared to the full panel. The model did not consider the reinforcing effect of screws to the wood, which strengthened the joint and also changed the failure mode, as observed in Phase I. The framework used in the model may also work with similar joints, like glued-in rods, for beam connections.

In the H-block test, screws were perpendicular to the grain of the surface layers. As the screws were pulled out in withdrawal mode, tension perpendicular to grain failure occurred in the surface layer, and the glue line between the surface layer and second layer delaminated. This phenomenon requires further study since this screw arrangement is not uncommon in practice. The effects of screw diameter, screw length, screw angle, screw arrangement, and washer types are under further investigation. Preliminary results showed that a smaller angle, for example 30° compared to 45° , led to a higher stiffness.

Since the connection could achieve the same level of stiffness in the minor direction as an intact panel, concrete topping (if necessary) will be designed using the common method. Bringing the concrete topping into resisting the bending moment, by providing additional compressive reaction and changing the location of the neutral axis, may be useful to certain extent. But first that leads to greater demand on the shear transfer between CLT and concrete layer. More importantly, the tension resistance remains to be solely supplied by the steel/LVL plates at the bottom. The improvement may not be significant enough to justify this approach.

4.2 Diaphragm behavior

The diaphragm test evaluated the performance of connectors under in-plane shear loading. The stiffness of the connectors was measured as the force applied to create a unit displacement between two adjacent CLT plates. There were two stiffness stages: the initial stage with a high stiffness, 56.8 kN/mm on average; and it transitioned to a prolonged low stiffness period with an average of 4.3 kN/mm. The transitional load was at the level of 16-27 kN. This trend was also found in some other cases with screws under lateral load at 90° to the loading direction. The high stiffness region is recommended for design use. Due to the number of connectors over per unit length of joint, the continuous CLT plate remains to be a fairly rigid plate with little energy dissipation in the plate plane. The damper devices tested in TEAM Report 2018-08 may be employed to mitigate that problem.

The critical part in the design may not be within the diaphragm itself, but between the diaphragm and other structural members, especially if column supported. Under lateral loading, the connection between the column and CLT plate will govern the design as a result of the high rigidity of the plate. As the size of the panel increases, the bearing capacity of CLT at the top of beams or columns will also become a major concern since that is controlled by the compressive strength perpendicular to grain. Special bearing plates and local reinforcements are necessary to address these issues.

4.3 Joined panel deflection

In Phase I and Phase II, four two way CLT panels were tested to measure the deflection at different locations. They had the same length in the major direction, and the single panels had half of the length of the joined panels in the minor direction. The panels were column supported at the four corners, with the out of plane load applied at the center. By doubling the length in the minor direction, the maximum deflection at the center also doubled, from an average of 5.87 mm to 12.00 mm. The principle deflection changed from the major direction to the minor direction. Attaching two PSL rim beams along the minor direction reduced the maximum deflection from 12.00 mm to 9.49 mm, a reduction of 21%, which corresponded to the increment of EI in the minor direction. If the concentrated load was uniformly distributed over the surface, the equivalent pressure would be 3.45 kPa. The deflection/span ratio was 1/280 for the joined panel, and 1/354 for the joined panel with rim beams.

A model using the crossing beam method was proposed to estimate the panel deflection at the center under a concentrated load. The principle direction, in which the main deflection occurred, was identified by comparing the $(EI)_{eff}$ and span of the two directions. The beam strip was in the principle direction, and the column strip was in the non-principle direction. The deflection was calculated using simple beam theory. The total deflection was the sum of the deflection in the two directions. The estimated deflection was in the range of 87-108% of the measured deflection. It also predicted the effect of rim beams well. Due to the limited number of tests, the model based on crossing beam method requires further validation by considering other length/width ratios and loading conditions. This method works better for uniformly distributed load than for concentrated load, according to its application in concrete two way slabs. Although uniformly distributed load is the common design condition, concentrated load is often used in the testing as limited by the panel size. An ongoing work is using Finite Element Method to simulate the deflection of two way continuous CLT plates. The data collected in Phase I and Phase II of this project was used to validate the model. Preliminary results indicated the model could predict the deflection of single panels within 5% of the measured values, but the current model was too sensitive to the support parameters and needed more adjustments.

4.4 Assembling and lifting

The dimensions of a large continuous two way CLT plate often exceed the size limit for common transportation, which means the connections have to be installed on site. The technique used in this project could be scaled up for that purpose, involving the following procedures:

1. A rigid platform is built from steel beams or glulam with spacers in between. The beams shall be parallel to the minor direction of the panels. The single CLT plates are then

placed on the platform which sits on a leveled surface. The ends of the beams are attached to the crane.

2. The gaps between CLT plates are closed using tie-straps, clamps or similar devices. Although the connectors have a capacity to pull the plates together, large gaps shall be avoided since that would compromise the joint stiffness.

3. Half of the connectors at the top (evenly spaced over the length) are installed first, then all the bottom connections, and in the end the other half at the top. Finishing one side at once may cause the joined panel to bow towards the other direction. The tie-straps or clamps shall remain in position until all connectors are installed.

4. The joined panel can be lifted to its structural position using this platform or common CLT lifting devices.

5 ACKNOWLEDGEMENTS

This project was financially supported by Forestry Innovation Investment. The material support from Structurlam Products Ltd. is gratefully acknowledged.

6 REFERENCES

TEAM Report 2017-08 *Connection and performance of two-way CLT plate*. C Zhang, G Lee, and F Lam. Report submitted to Forestry Innovation Investment BC. April 6, 2018.

TEAM Report 2018-08 *Connections for stackable heavy timber modules in midrise to tall wood buildings*. C Zhang, G Lee, and F Lam. Report submitted to Forestry Innovation Investment BC. March 31, 2019.

Appendix A Joined panel test results

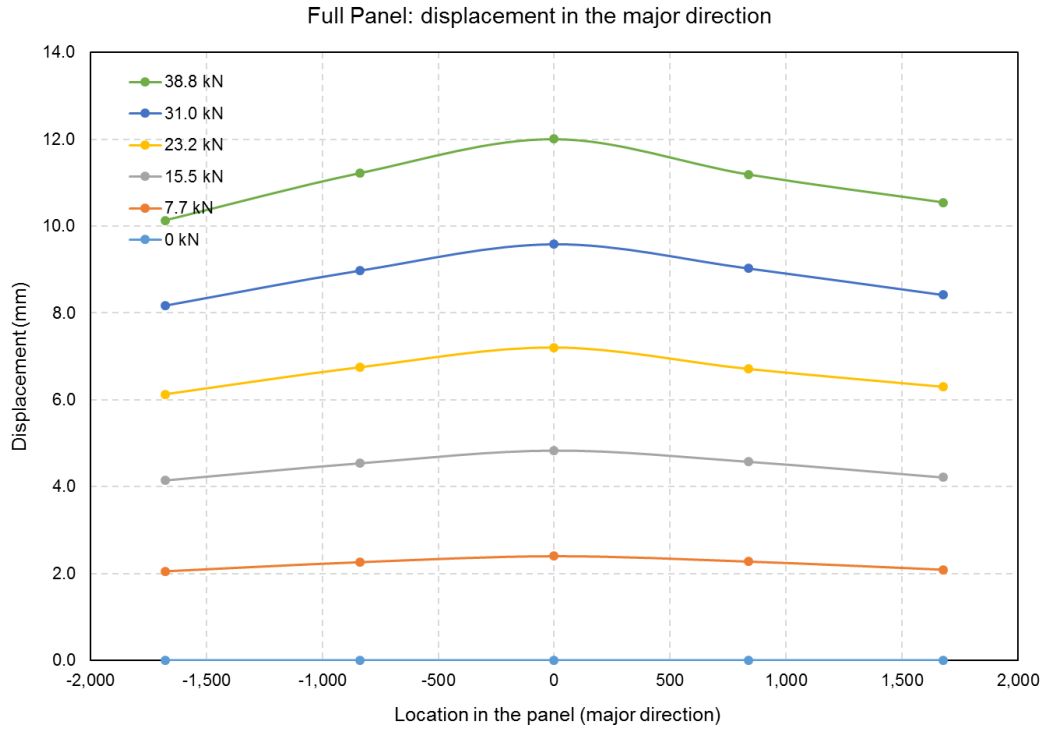


Figure A- 1 Displacement of the joined panel in the major direction

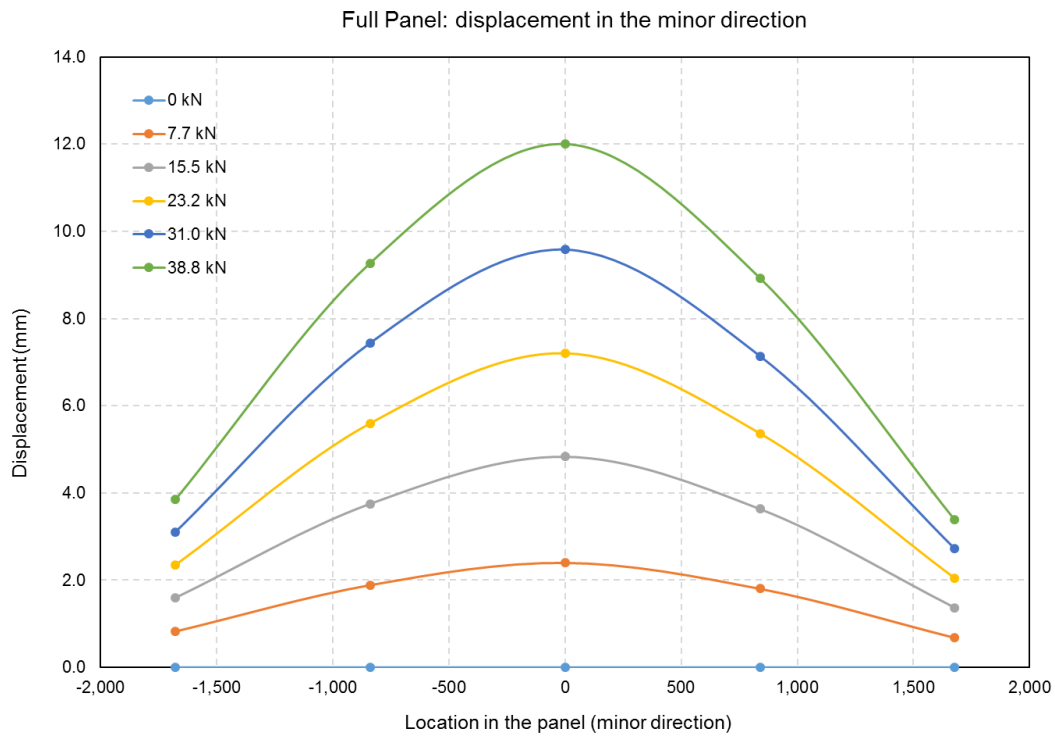


Figure A- 2 Displacement of the joined panel in the minor direction

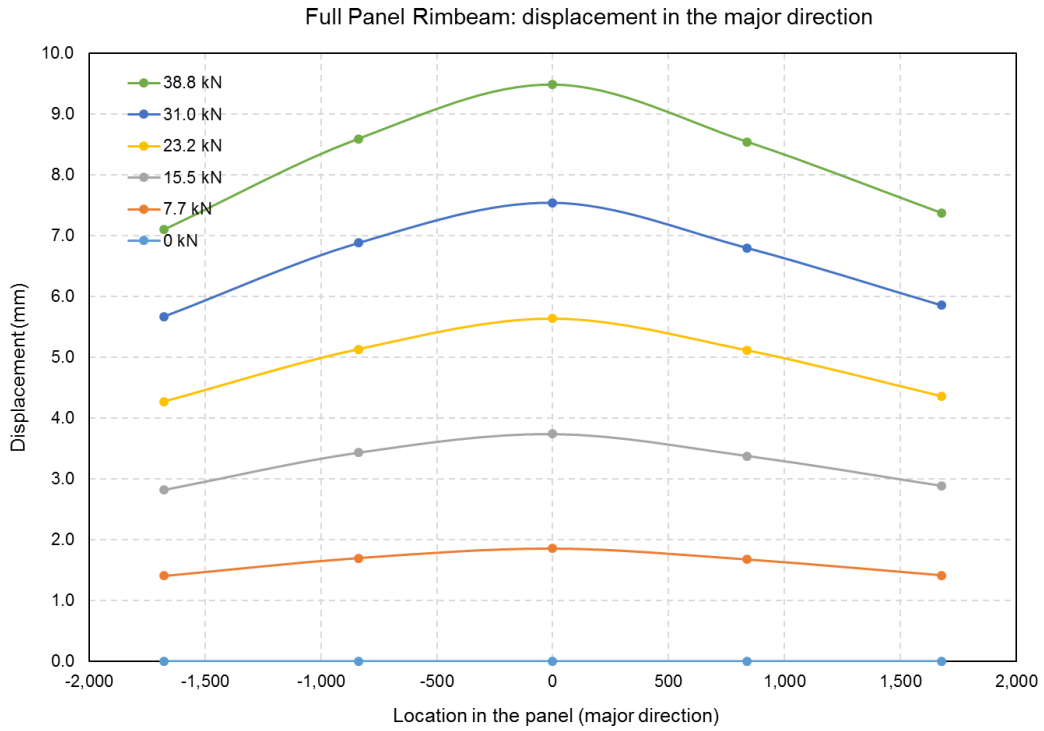


Figure A- 3 Displacement of the joined panel with rim beams in the major direction

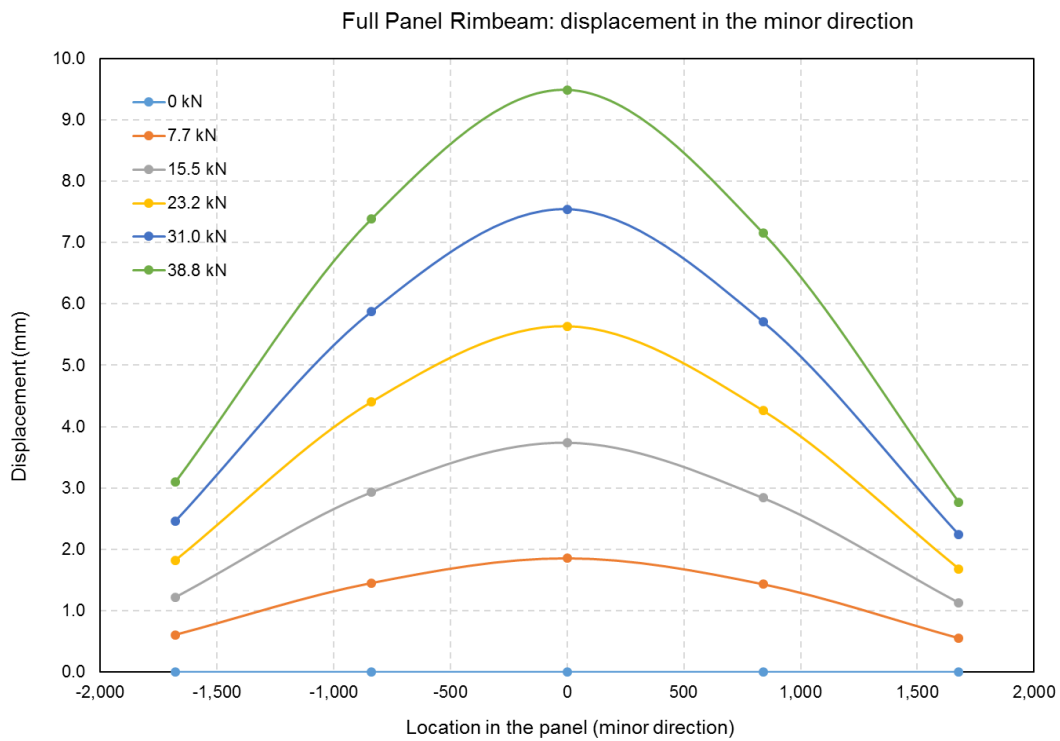


Figure A- 4 Displacement of the joined panel with rim beams in the minor direction

THE END